

$\mathcal{O}(\alpha_s)$ corrections to the B-hadron energy distribution of the top decay in the general two Higgs doublet model considering GM-VFN scheme

S. Mohammad Moosavi Nejad^{a,b}

^a*Faculty of Physics, Yazd University, P.O. Box 89195-741, Yazd, Iran*

^b*School of Particles and Accelerators, Institute for Research in Fundamental Sciences (IPM), P.O.Box 19395-5531, Tehran, Iran*

E-mail: mmoosavi@yazduni.ac.ir

ABSTRACT: We present our analytic results for the NLO corrections to the partial decay width $t \rightarrow H^+b$ followed by $b \rightarrow BX$ for nonzero b-quark mass ($m_b \neq 0$) in the Fixed-Flavor-Number scheme (FFNs). To make our predictions for the energy distribution of the outgoing bottom-flavored hadron (B-hadron) as a function of the normalized B-energy fraction x_B , we apply the General-Mass Variable-Flavor-Number scheme (GM-VFNs) in the general two-Higgs-doublet model. In order to describe both the b-quark and the gluon hadronizations in top decay we use fragmentation functions extracted from data from e^+e^- machines. We find that the most reliable prediction for the B-hadron energy spectrum is made in the GM-VFN scheme.

PACS numbers: 14.65.Ha, 13.85.Ni, 14.40.Nd, 14.80.Da

Contents

1	Introduction	1
2	Parton level results	2
2.1	Born level rate of $t \rightarrow bH^+$	2
2.2	Virtual one-loop corrections and counterterms	4
2.3	Real one-loop corrections (Bremsstrahlung)	6
2.4	Parton-level results for $d\tilde{\Gamma}/dx_a$ in FFN scheme	6
3	GM-VFN scheme	7
4	Numerical results	8
5	Conclusions	13

1 Introduction

The top quark has been the latest standard model particle discovered by the CDF and D0 experiments at Fermilab Tevatron [1]. Its properties are essential for our understanding of the standard model (SM) theory. At the Large Hadron Collider (LHC), one expects a cross section $\sigma(pp \rightarrow t\bar{t}X) \approx 1$ (nb) at design energy $\sqrt{S} = 14$ TeV [2]. With the LHC design luminosity of $10^{34}(cm)^{-2}(sec)^{-1}$, it is expected to produce a $t\bar{t}$ pair per second. Thus, the LHC is a superlative top factory, which allows to carry out precision tests of the SM and, specifically a precise measurement of the top quark properties such as its mass. Due to the element $|V_{tb}| \approx 1$ of the Cabibbo-Kobayashi-Maskawa (CKM) [3] quark mixing matrix, the top quark is decaying dominantly through the mode $t \rightarrow bW^+$ within the SM. As it is well known, bottom quarks hadronize before they decay, therefore each b-jet contains a B-hadron which most of the times is a B-meson. Events with B-mesons are identified by a displaced decay vertex associated which charged-lepton tracks. This is precisely the signature used to identify b-jets. In Ref. [4], we studied the B-meson energy distribution produced in top decay considering both the bottom quark and the gluon fragmentations. We also studied the angular distribution of the W-boson decay products in the decay chain $t \rightarrow bW^+ \rightarrow Bl^+\nu_l + X$. The effects of b-quark and hadron masses are also considered.

In many extensions of the SM such as the minimal supersymmetric standard model (MSSM), the Higgs sector of the SM is enlarged, typically by adding an extra doublet of complex Higgs fields. After spontaneous symmetry breaking, the two scalar Higgs doublets H_1 and H_2 yield three physical neutral Higgs bosons (h, H, A) and a pair of charged-Higgs bosons (H^\pm) [5]. The top quark is decaying dominantly through $t \rightarrow bH^+$ in a model with two-Higgs-doublet (2HDM) [6], providing that the top quark mass m_t , bottom

quark mass m_b and the charged-Higgs boson mass m_H^+ satisfy $m_t > m_b + m_H^+$. In this case one expects measurable effects in the top quark decay width and decay distributions due to the H^\pm -propagator contributions, which are potentially large in the decay chain $t \rightarrow bH^+ \rightarrow b(\tau^+\nu_\tau)$.

At LHC, the dominant source of top quarks is $pp \rightarrow t\bar{t}$ process, therefore the charged Higgs boson has been searched for in the subsequent decay products of the top pairs $t\bar{t} \rightarrow H^\pm W^\mp b\bar{b}$ and $t\bar{t} \rightarrow H^\pm H^\mp b\bar{b}$ when H^\pm decays into τ lepton and neutrino.

In our previous work [7], we studied the energy spectrum of the inclusive bottom-flavored mesons in the presence of charged Higgs boson by working in the massless scheme or zero-mass variable-flavor-number (ZM-VFN) scheme where the mass of bottom quark is set to zero from the beginning. As it was shown, in the limit of vanishing b-quark mass our results in two variants of the 2HDM are the same. In the present work, we impose the effect of b-quark mass on the B-spectrum employing the general-mass variable-flavor-number (GM-VFN) scheme. As it is shown, the results will be different in two variants of the 2HDM and it is found the NLO corrections with $m_b \neq 0$ to be significant.

To obtain the total B-hadron energy distribution of the top decay, two contributions due to the decay modes $t \rightarrow bW^+$ (in the SM) and $t \rightarrow bH^+$ (in the 2HDM) should be summed up. However, the contribution of SM is always larger than the one coming from 2HDM [7], but there is a clear separation between the decay channels $t \rightarrow bW^+$ and $t \rightarrow bH^+$ in both the $t\bar{t}X$ pair production and the $t/\bar{t}X$ single top production at the LHC [8]. New results of a study on the charged-Higgs bosons in pp collision at a center of mass energy of $\sqrt{s} = 7$ TeV are reported by the ATLAS Collaboration [9].

Finally, since bottom quarks fragment into the B-meson, in order to describe the b-quark non-perturbative fragmentation some phenomenological hadronization models can be used. Our treatment at NLO in the GM-VFN scheme is manifestly based on the factorization theorem of QCD which guarantees that the fragmentation functions are universal and subject to DGLAP evolutions [10]. Relying on the universality of the hadronization mechanism, we can tune such models to data on B production in e^-e^+ annihilation data from CERN LEP1 and SLAC SLC and use them to predict the B-hadron spectrum in top decay. The hadronization of the b-quark was considered in the NLO QCD analysis of top-quark decay in Refs. [11, 12] and was identified to be the most important factor of uncertainty in the determination of the top-quark mass.

This paper is organized as follows. In Sec. 2, we give the parton-level expressions for the NLO QCD corrections to the tree-level rate of $t \rightarrow bH^+$ in the fixed flavor number (FFN) scheme. In Sec. 3, the scheme of GM-VFN is explained by introducing the perturbative fragmentation function $b \rightarrow b$. In Sec. 4, we present our hadron-level results working in the GM-VFN scheme. In Sec. 5, we summarize our conclusions.

2 Parton level results

2.1 Born level rate of $t \rightarrow bH^+$

We consider the decay channel $t \rightarrow bH^+$ in the general 2HDM, where H_1 and H_2 are the doublets whose vacuum expectation values give masses to the down and up type quarks,

respectively, and a linear combination of the charged components of H_1 and H_2 gives the physical charged Higgs H^+ . In a general model with two Higgs doublets to avoid tree level flavor-changing neutral currents (FCNC), the generic Higgs coupling to all quarks has to be restricted. There are two possibilities for the two Higgs doublets to couple to the fermions. In the first possibility (model I), one of the Higgs doublets (H_1) couples to all bosons and the other one (H_2) couples to all the quarks. In this model, the Yukawa couplings between the charged Higgs boson, the top and the bottom quarks are given by [13]

$$L_I = \frac{g_W}{2\sqrt{2}m_W} V_{tb} \cot \beta \left\{ H^+ \bar{t} [m_t(1 - \gamma_5) - m_b(1 + \gamma_5)] b \right\} + H.c. \quad (2.1)$$

For the vacuum expectation values of $H_1(\mathbf{v}_1)$ and $H_2(\mathbf{v}_2)$, we have $\mathbf{v}_1^2 + \mathbf{v}_2^2 = (\sqrt{2}G_F)^{-1}$ where G_F is the Fermi's constant and the ratio of the two values is a free parameter and one can define the angle β to parameterize it, i.e. $\tan \beta = \mathbf{v}_2/\mathbf{v}_1$. The weak coupling factor g_W is related to the Fermi coupling constant by $g_W^2 = 4\sqrt{2}m_W^2 G_F$. In the equation above, $H^+ = \cos \beta H_2^+ - \sin \beta H_1^+$ is the physical charged Higgs boson.

In the second possibility (model II), the doublet H_2 couples to the right-handed up-type quarks (u_R, c_R, t_R) and the H_1 couples to the right-handed down-type quarks. In this model, the interaction Lagrangian would be

$$L_{II} = \frac{g_W}{2\sqrt{2}m_W} V_{tb} \left\{ H^+ \bar{t} [m_t \cot \beta (1 - \gamma_5) + m_b \tan \beta (1 + \gamma_5)] b \right\} + H.c. \quad (2.2)$$

The Born amplitude for the process $t \rightarrow bH^+$ can be parameterized as $M_0 = \bar{u}_b(a + b\gamma_5)u_t$, therefore, the tree-level total decay width is given by

$$\tilde{\Gamma}_0 = \frac{m_t}{16\pi} \left\{ (a^2 + b^2) \left[1 + \frac{m_b^2}{m_t^2} - \frac{m_{H^+}^2}{m_t^2} \right] + 2(a^2 - b^2) \frac{m_b}{m_t} \right\} \lambda^{\frac{1}{2}}(1, \frac{m_b^2}{m_t^2}, \frac{m_{H^+}^2}{m_t^2}), \quad (2.3)$$

where $\lambda(x, y, z) = (x - y - z)^2 - 4yz$ is the Källén function and for model I, one has

$$\begin{aligned} a^2 + b^2 &= \sqrt{2}|V_{tb}|^2 G_F (m_t^2 + m_b^2) \cot^2 \beta, \\ a^2 - b^2 &= -2\sqrt{2}|V_{tb}|^2 G_F (m_b m_t) \cot^2 \beta, \end{aligned} \quad (2.4)$$

and for model II

$$\begin{aligned} a^2 + b^2 &= \sqrt{2}|V_{tb}|^2 G_F (m_t^2 \cot^2 \beta + m_b^2 \tan^2 \beta), \\ a^2 - b^2 &= 2\sqrt{2}|V_{tb}|^2 G_F (m_b m_t). \end{aligned} \quad (2.5)$$

In the limit of vanishing b-quark mass, the tree level decay width is discussed in [7]. Since $m_b \ll m_t$, the b-quark mass can always be safely neglected in model I but in model II, the left-chiral coupling term proportional to $m_b \tan \beta$ can become comparable to the right-chiral coupling term $m_t \cot \beta$ when $\tan \beta$ becomes large. Therefore, one can not naively set $m_b = 0$ in all expressions in model II.

In the following, we explain the calculation of the NLO QCD corrections to the Born level decay rate of $t \rightarrow bH^+$ and we present the parton-level expressions for $d\Gamma(t \rightarrow BH^+ + X)/dx_B$ at NLO in the FFN scheme where $m_b \neq 0$ is considered.

2.2 Virtual one-loop corrections and counterterms

The virtual corrections to the tbH^+ -vertex consists of both infrared (IR) and ultraviolet (UV) singularities where the ir- and uv-divergences arise from the collinear- and the soft-gluon singularities, respectively. In our calculation, we adopt the on-shell mass-renormalization scheme and all singularities are regularized by dimensional regularization in $D = 4 - 2\epsilon$ space-time dimensions. To simplify the formulas we introduce the following kinematic variables, in the notation of Refs. [14, 15], along with some other required variables

$$\begin{aligned}
p_0 &= \frac{1}{2}(1 + R - y), \\
\beta &= \frac{\sqrt{R}}{p_0}, \\
p_3 &= p_0 \sqrt{1 - \beta^2}, \\
p_{\pm} &= p_0 \pm p_3, \\
Y_p &= \frac{1}{2} \ln \frac{p_+}{p_-}, \\
Y_w &= \frac{1}{2} \ln \frac{1 - p_-}{1 - p_+}, \\
H &= (a^2 + b^2)p_0 + (a^2 - b^2)\sqrt{R}, \\
T &= p_0(1 - x_b)\sqrt{x_b^2 - \beta^2}, \\
\Phi(x_b) &= p_0 \left[\sqrt{x_b^2 - \beta^2} - \ln \frac{\beta}{x_b - \sqrt{x_b^2 - \beta^2}} \right], \tag{2.6}
\end{aligned}$$

where the scaled masses $R = m_b^2/m_t^2$ and $y = m_{H^+}^2/m_t^2$ are defined. Choosing these notations, the tree-level total width (Eq. (2.3)) is simplified to $\tilde{\Gamma}_0 = m_t H p_3 / (4\pi)$. It is also convenient to introduce the normalized energy fractions $x_i = E_i/E_b^{max}$ ($i = b, g$) where $E_b^{max} = m_t p_0$.

Considering the above notations, the contribution of virtual corrections into the differential decay width reads

$$\frac{d\tilde{\Gamma}_b^{\text{vir}}}{dx_b} = \frac{p_3}{8\pi m_t} \overline{|M^{\text{vir}}|^2} \delta(1 - x_b), \tag{2.7}$$

where, $\overline{|M^{\text{vir}}|^2} = 1/2 \sum_{Spin} (M_0^\dagger M_{loop} + M_{loop}^\dagger M_0)$. The renormalized amplitude of the virtual corrections is written as $M_{loop} = \bar{u}_b(\Lambda_{ct} + \Lambda_l)u_t$, where Λ_{ct} stands for the counter term and Λ_l arises from the one-loop vertex correction. Following Refs. [14–16], the counter term of the vertex includes the mass and the wave-function renormalizations of both the top and bottom quarks as

$$\Lambda_{ct} = (a + b) \left(\frac{\delta Z_b}{2} + \frac{\delta Z_t}{2} - \frac{\delta m_t}{m_t} \right) \frac{1 + \gamma_5}{2} + (a - b) \left(\frac{\delta Z_b}{2} + \frac{\delta Z_t}{2} - \frac{\delta m_b}{m_b} \right) \frac{1 - \gamma_5}{2}, \tag{2.8}$$

where, the mass and the wave function renormalization constants read

$$\begin{aligned}\frac{\delta m_q}{m_q} &= \frac{\alpha_s(\mu_R)}{4\pi} C_F \left(\frac{3}{\epsilon_{UV}} - 3\gamma_E + 3 \ln \frac{4\pi\mu_F^2}{m_q^2} + 4 \right), \\ \delta Z_q &= -\frac{\alpha_s(\mu_R)}{4\pi} C_F \left(\frac{1}{\epsilon_{UV}} + \frac{2}{\epsilon_{IR}} - 3\gamma_E + 3 \ln \frac{4\pi\mu_F^2}{m_q^2} + 4 \right).\end{aligned}\quad (2.9)$$

Here, m_q is the mass of the relevant quark and $C_F = (N_c^2 - 1)/(2N_c) = 4/3$ for $N_c = 3$ quark colors. In the equation above, ϵ_{IR} and ϵ_{UV} represent infrared and ultraviolet singularities and $\gamma_E = 0.577216 \dots$ stands for the Euler constant.

The real part of the one-loop vertex correction reads

$$\Lambda_l = \frac{\alpha_s m_t^2}{\pi} C_F [(a^2 - b^2)\sqrt{R}G_+ + (a^2 + b^2)G_-], \quad (2.10)$$

with

$$\begin{aligned}G_+ &= 4m_t^2 p_0 C_0(m_b^2, m_t^2, m_{H^+}^2, m_b^2, 0, m_t^2) + B_0(m_b^2, 0, m_b^2) + 2B_0(m_{H^+}^2, m_b^2, m_t^2) \\ &\quad + B_0(m_t^2, 0, m_t^2) - 2, \\ G_- &= 4m_t^2 p_0^2 C_0(m_b^2, m_t^2, m_{H^+}^2, m_b^2, 0, m_t^2) + (2p_0 - R)B_0(m_b^2, 0, m_b^2) \\ &\quad + (1 + R)B_0(m_{H^+}^2, m_b^2, m_t^2) + (2p_0 - 1)B_0(m_t^2, 0, m_t^2) - 2p_0,\end{aligned}\quad (2.11)$$

where, B_0 and C_0 functions are the Passarino-Veltman 2-point and 3-point integrals which can be found in Ref. [17].

All uv-singularities are canceled after summing all virtual corrections up but the ir-divergences are remaining which are now labeled by ϵ . Putting everything together, the virtual differential decay rate normalized to the Born total width, reads

$$\begin{aligned}\frac{1}{\tilde{\Gamma}_0} \frac{d\tilde{\Gamma}_b^{\text{vir}}}{dx_b} &= \frac{\alpha_s(\mu_R)}{2\pi} C_F \delta(1 - x_b) \left\{ -2 + \ln R \left[\frac{2(1 - p_0)}{y} - \frac{3abp_0}{H} - \frac{2p_0}{p_3} (Y_p + Y_w) \right] \right. \\ &\quad \left. - \frac{2p_0}{p_3} Y_p \left(Y_p - \ln y - \frac{p_3^2}{yp_0 H} [2\sqrt{R}(a^2 - b^2) + (a^2 + b^2)(1 + R)] \right) \right. \\ &\quad \left. - 2 \left[1 - \frac{p_0}{p_3} Y_p \right] \left(\ln \frac{4\pi\mu_F^2}{m_t^2} - \gamma_E + \frac{1}{\epsilon} \right) - \frac{2p_0}{p_3} \left[Li_2(p_-) - Li_2(p_+) + Li_2\left(1 - \frac{p_-}{p_+}\right) \right] \right\},\end{aligned}\quad (2.12)$$

where, $Li_2(x) = -\int_0^x (dt/t) \ln(1 - t)$ is the Spence function. In Eq. (2.12), one has

$$ab = \frac{G_F}{\sqrt{2}} |V_{tb}|^2 (m_t^2 - m_b^2) \cot^2 \beta, \quad (2.13)$$

in model I, and

$$ab = \frac{G_F}{\sqrt{2}} |V_{tb}|^2 (m_t^2 \cot^2 \beta - m_b^2 \tan^2 \beta), \quad (2.14)$$

in model II. The terms $a^2 + b^2$ and $a^2 - b^2$ are given in Eqs. (2.4) and (2.5) in both models.

2.3 Real one-loop corrections (Bremsstrahlung)

The $\mathcal{O}(\alpha_s)$ real gluon emission amplitude reads

$$M^{tree} = g_s \frac{\lambda^a}{2} \bar{u}(p_b, s_b) \left\{ \frac{2p_t^\mu - \not{p}_g \gamma^\mu}{2p_t \cdot p_g} - \frac{2p_b^\mu + \gamma^\mu \not{p}_g}{2p_b \cdot p_g} \right\} (a + b\gamma_5) u(p_t, s_t) \epsilon_\mu^*(p_g, r), \quad (2.15)$$

where the polarization vector of the gluon is denoted by $\epsilon(p_g, r)$. As before, to regulate the IR-divergences we work in $D = 4 - 2\epsilon$ dimensions and for simplicity, we choose the top quark rest-frame. To get the correct finite terms in the normalized differential decay rate, the Born width $\tilde{\Gamma}_0$ will have to be evaluated in the dimensional regularization at $\mathcal{O}(\epsilon)$, i.e. $\tilde{\Gamma}_0 \rightarrow \tilde{\Gamma}_0 \{1 - \epsilon [2 \ln(2p_3) + \gamma_E - \ln(4\pi\mu^2/m_t^2) - 2]\}$. When one integrates over the phase space for the real-gluon radiation, terms of the form $(1 - x_b)^{-1-2\epsilon}$ arise which are due to the radiation of a soft gluon in top decay. Therefore, for a massive b quark, where $x_{b,min} = \beta$, we use the following expansion

$$\frac{(x_b - \beta)^{2\epsilon}}{(1 - x_b)^{1+2\epsilon}} = -\frac{1}{2\epsilon} \delta(1 - x_b) + \frac{1}{(1 - x_b)_+} + \mathcal{O}(\epsilon), \quad (2.16)$$

where the plus distribution is defined as

$$\int_\beta^1 \frac{f(x_b)}{(1 - x_b)_+} dx_b = \int_\beta^1 \frac{f(x_b) - f(1)}{1 - x_b} dx_b + f(1) \ln(1 - \beta). \quad (2.17)$$

2.4 Parton-level results for $d\tilde{\Gamma}/dx_a$ in FFN scheme

Now, we present our analytic results for partial decay rate normalized to the Born width in the FFN scheme, by summing the tree level, the virtual and the real contributions. Our result reads

$$\begin{aligned} \frac{1}{\tilde{\Gamma}_0} \frac{d\tilde{\Gamma}_b}{dx_b} = & \delta(1 - x_b) + \frac{C_F \alpha_s(\mu_R)}{\pi} \left\{ \delta(1 - x_b) \left[\frac{(1 - R)Y_w}{p_3} - 2 \ln \frac{2p_0 p_+}{\sqrt{y}} - 1 \right. \right. \\ & - 2 \frac{p_0}{p_3} [Li_2(p_-) - Li_2(p_+) + Li_2(1 - \frac{p_-}{p_+})] + 2 \frac{Y_p}{p_3} \left(p_3 + \frac{p_0 - R}{2} + p_0 \ln \frac{2p_0 \sqrt{y}}{p_+} + \right. \\ & \left. \left. \frac{p_3^2}{2yH} [2(a^2 - b^2)\sqrt{R} + (1 + R)(a^2 + b^2)] \right) + \left(\frac{1 + y - p_0}{y} - \frac{p_0}{p_3} Y_w - \frac{3p_0}{2H} ab \right) \ln R \right] \\ & \left. - \frac{2(T + x_b \Phi(x_b))}{Hp_3(1 - x_b)_+} [\sqrt{R}(a^2 - b^2) + (a^2 + b^2)p_0 x_b] - p_0 \frac{a^2 + b^2}{Hp_3} [T + (1 + x_b)\Phi(x_b)] \right\}. \end{aligned} \quad (2.18)$$

Integrating $d\tilde{\Gamma}_b/dx_b$ of Eq. (2.18) over $x_b(\beta < x_b < 1)$, we obtain the total decay rate presented in Refs. [14, 15].

Since, the B-meson can be also produced from the fragmentation of the emitted real gluon, we also need the differential decay rate $d\tilde{\Gamma}_g/dx_g$ in the FFN scheme, where $x_g = E_g/(m_t p_0)$ is the scaled energy fraction of the real gluon. To calculate the $d\tilde{\Gamma}_g/dx_g$, we

integrate over the momentum of b-quark by fixing the momentum of gluon in the phase space. Our result is listed here

$$\begin{aligned} \frac{1}{\tilde{\Gamma}_0} \frac{d\tilde{\Gamma}_g}{dx_g} = & \frac{C_F \alpha_s(\mu_R) p_0^2 (1-x_g)}{\pi p_3 x_g H} \left\{ \left[(a^2 + b^2) \left(1 - x_g + \frac{1}{1-x_g} \right) + 2\beta(a^2 - b^2) \right] \right. \\ & \times \tanh^{-1} \sqrt{1 - \frac{\beta^2(1-2p_0x_g)}{(1-x_g)^2}} - \left[(a^2 + b^2) \left(2 + \frac{p_0x_g^2[2-p_0(1+3x_g)]}{(1-2p_0x_g)^2} \right) \right. \\ & \left. \left. + 2\beta(a^2 - b^2) \right] \sqrt{1 - \frac{\beta^2(1-2p_0x_g)}{(1-x_g)^2}} \right\}. \end{aligned} \quad (2.19)$$

3 GM-VFN scheme

Our main purpose is to calculate the scaled-energy distribution of the B-hadron produced in the inclusive process $t \rightarrow BH^+ + X$ in the 2HDM, where X stands for the unobserved final state. Thus we calculate the partial decay width of the corresponding process differential in x_B ($d\Gamma/dx_B$), at NLO in the GM-VFN scheme, where $x_B = E_B/(m_t p_0)$ is the scaled energy fraction of the B-hadron. In the top quark rest frame, the B-hadron has energy $E_B = p_t \cdot p_B/m_t$, where $m_B \leq E_B \leq [m_t^2 + m_B^2 - m_{H^+}^2]/(2m_t)$. In the case of gluon fragmentation, $g \rightarrow B$, it has energy $m_B \leq E_B \leq [m_t^2 + m_B^2 - (m_b + m_{H^+})^2]/(2m_t)$. According to the factorization theorem of QCD [18], the B-hadron energy distribution can be obtained by the convolution of the parton-level spectrum with the nonperturbative fragmentation function $D_a^B(z, \mu_F)$,

$$\frac{d\Gamma}{dx_B} = \sum_{a=b,g} \int_{x_a^{\min}}^{x_a^{\max}} \frac{dx_a}{x_a} \frac{d\Gamma_a^{GM}}{dx_a}(\mu_R, \mu_F) D_a^B\left(\frac{x_B}{x_a}, \mu_F\right),$$

where, μ_F is the factorization scale and μ_R is the renormalization scale which is related to the renormalization of the QCD coupling constant. A choice often made is to set $\mu_R = \mu_F$ and we shall use this convention for most of the results. Here, $d\Gamma_a^{GM}/dx_a$ is the differential decay width of the parton-level process $t \rightarrow a + X$ at NLO in the GM-VFN scheme, where X comprising the H^+ boson and any other parton. We now discuss the evaluation of the quantities $d\Gamma_a^{GM}(\mu_R, \mu_F)/dx_a$ in the GM-VFN scheme in detail.

In Ref. [7], using the ZM-VFN scheme we evaluated the quantities $1/\Gamma_0 \times d\tilde{\Gamma}_a/dx_a$ ($a = b, g$) for the process $t \rightarrow a + X$, where $m_b = 0$ is put right from the beginning. In this scheme, m_b only sets the initial scale $\mu_F^{ini} = \mathcal{O}(m_b)$ of the DGLAP evolution, however all information on the m_b dependence of $d\tilde{\Gamma}_a/dx_a$ is wasted.

In sec. 2 of the present paper, we applied the FFN scheme which contains of the full m_b dependence. In this scheme, the large logarithmic singularities of the type $(\alpha_s/\pi) \ln R$, where $R = m_b^2/m_t^2$, spoil the convergence of the perturbative expansion when $m_b/m_t \rightarrow 0$ (see Eq. (2.18)). The GM-VFN scheme is devised to resum the large logarithms in m_b and to retain the whole nonlogarithmic m_b dependence at the same time. This is achieved by introducing appropriate subtraction terms in the NLO FFN expressions for $d\tilde{\Gamma}_a/dx_a$, so that the NLO ZM-VFN results are exactly recovered in the limit $m_b/m_t \rightarrow 0$. With this

explanation, the subtraction terms are constructed as

$$\frac{1}{\Gamma_0} \frac{d\Gamma_a^{Sub}}{dx_a} = \lim_{m_b \rightarrow 0} \frac{1}{\Gamma_0} \frac{d\tilde{\Gamma}_a^{FFN}}{dx_a} - \frac{1}{\Gamma_0} \frac{d\hat{\Gamma}_a^{ZM}}{dx_a}, \quad (3.1)$$

and the GM-VFN results are obtained by subtracting the subtraction terms from the FFN ones [19, 20], as

$$\frac{1}{\Gamma_0} \frac{d\Gamma_a^{GM}}{dx_a} = \frac{1}{\Gamma_0} \frac{d\tilde{\Gamma}_a^{FFN}}{dx_a} - \frac{1}{\Gamma_0} \frac{d\Gamma_a^{Sub}}{dx_a}. \quad (3.2)$$

Taking the limit $m_b \rightarrow 0$ in Eqs. (2.18) and (2.19), we obtain the subtraction terms as

$$\frac{1}{\Gamma_0} \frac{d\Gamma_b^{Sub}}{dx_b} = \frac{\alpha_s(\mu_R)}{2\pi} C_F \left\{ \frac{1+x_b^2}{1-x_b} \left[\ln \frac{\mu_F^2}{m_b^2} - 2 \ln(1-x_b) - 1 \right] \right\}_+, \quad (3.3)$$

$$\frac{1}{\Gamma_0} \frac{d\Gamma_g^{Sub}}{dx_g} = \frac{\alpha_s(\mu_R)}{2\pi} C_F \frac{1+(1-x_g)^2}{x_g} \left(\ln \frac{\mu_F^2}{m_b^2} - 2 \ln x_g - 1 \right). \quad (3.4)$$

As it is guaranteed by Collin's factorization theorem [18], the subtraction terms are universal and as we already presented in Ref. [4], Eq. (3.3) coincides with the perturbative FF of the transition $b \rightarrow b$ [21].

4 Numerical results

Now we present our phenomenological predictions by performing a numerical analysis. As it is referred in Ref. [22], a charged Higgs having a mass in the range $80 \text{ GeV} \leq m_{H^\pm} \leq 160 \text{ GeV}$ is a logical possibility and its effects should be searched for in the decay modes $t \rightarrow bH^+ \rightarrow B\tau^+\nu_\tau + X$. A beginning along these lines has already been made at the Tevatron [23, 24], but a definitive search of the charged-Higgses over a good part of the $(m_{H^+} - \tan\beta)$ plane is a program that still has to be carried out and this belongs to the LHC experiments [25].

Following Ref. [26], we adopt the present lower limit $m_{H^+} > 79.3 \text{ GeV}$ obtained from LEP. From Ref. [26], we use the input parameter values $G_F = 1.16637 \times 10^{-5} \text{ GeV}^{-2}$, $m_t = 172.0 \text{ GeV}$, $m_b = 4.90 \text{ GeV}$, $m_B = 5.279 \text{ GeV}$, and $|V_{tb}| = 0.999152$. We evaluate $\alpha_s^{(n_f)}(\mu_R)$ at NLO in the $\overline{\text{MS}}$ scheme using

$$\alpha_s^{(n_f)}(\mu) = \frac{1}{b_0 \log(\mu^2/\Lambda^2)} \left\{ 1 - \frac{b_1 \log[\log(\mu^2/\Lambda^2)]}{b_0^2 \log(\mu^2/\Lambda^2)} \right\}, \quad (4.1)$$

with b_0 and b_1 given by

$$b_0 = \frac{33 - 2n_f}{12\pi}, \quad b_1 = \frac{153 - 19n_f}{24\pi^2}, \quad (4.2)$$

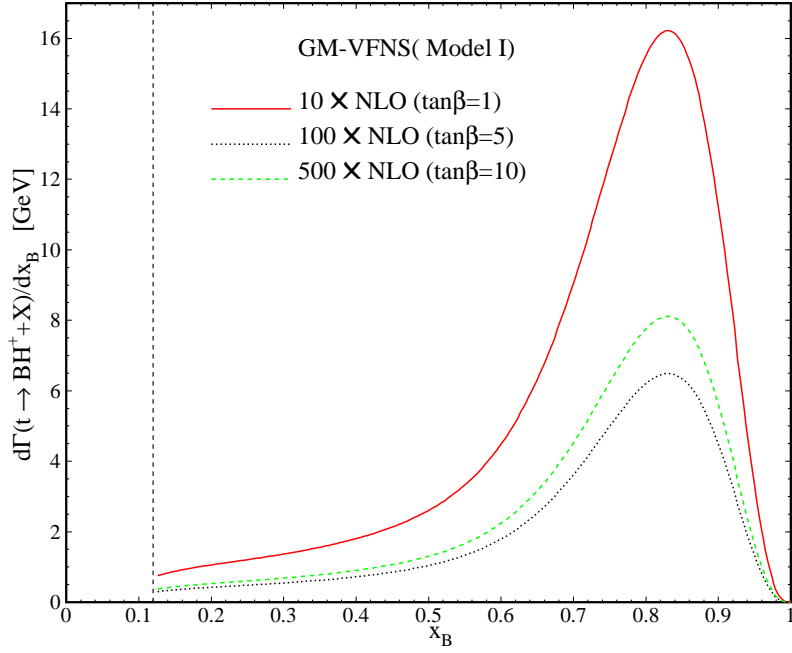


Figure 1. $d\Gamma(t \rightarrow BH^+ + X)/dx_B$ as a function of x_B in the GM-VFN scheme for model I, taking $m_{H^+} = 120$ GeV and $\tan\beta = 1, 5$ and 10 .

where Λ is the typical QCD scale and we adopt $\Lambda_{\overline{\text{MS}}}^{(5)} = 231.0$ MeV adjusted such that $\alpha_s^{(5)} = 0.1184$ for $m_Z = 91.1876$ GeV [26]. In Eq. (4.1), n_f is the number of active quark flavors.

To describe the transitions $b, g \rightarrow B$, we employ the realistic nonperturbative B -hadron FFs determined at NLO in the zero-mass scheme through a global fit to e^+e^- -annihilation data presented by ALEPH [27] and OPAL [28] at CERN LEP1 and by SLD [29] at SLAC SLC. Specifically, for the $b \rightarrow B$ transition the power model $D_b(z, \mu_F^{\text{ini}}) = N z^\alpha (1-z)^\beta$ was used at the initial scale $\mu_F^{\text{ini}} = 4.5$ GeV, while the light-quark and gluon FFs were generated via the DGLAP evolution. The result of fit read $N = 4684.1$, $\alpha = 16.87$, and $\beta = 2.628$ [30]. Note, if the same experimental data are fitted in the ZM-VFN and GM-VFN schemes, the resulting FFs will be somewhat different. As it is shown in Ref. [31], the hadronization of the bottom quark is identified to be the largest source of uncertainty in the measurement of the top quark mass.

To present our results for the scaled-energy (x_B) distribution of B -hadrons, we consider the quantity $d\Gamma(t \rightarrow BH^+ + X)/dx_B$ taking the H^+ boson to be stable. In Fig. 1, we show our prediction for the size of the NLO corrections in the GM-VFN scheme for the model I. Here, the mass of Higgs boson is fixed to $m_{H^+} = 120$ GeV and the different values of $\tan\beta$ are considered, i.e. $\tan\beta = 1, 5$ and 10 . However, as in Ref. [32] it is pointed out, the small values of $\tan\beta$ are excluded by the indirect limits in the $(m_{H^\pm}, \tan\beta)$ plane. For example, taking the CP-conserving scenario m_h -max and a top quark mass of 174.3 GeV, values of $\tan\beta$ between 0.7 and 2.0 are excluded, but this range depends considerably on

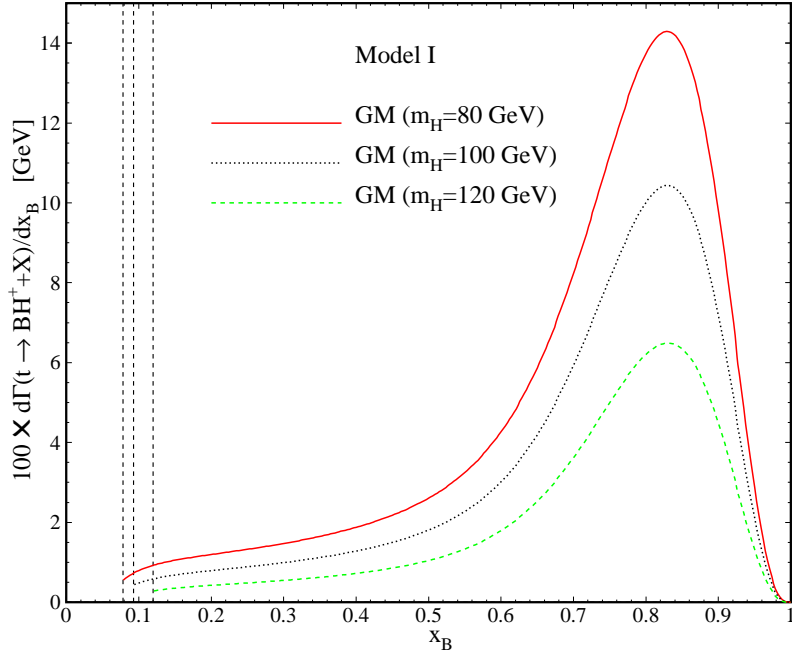


Figure 2. $d\Gamma(t \rightarrow BH^+ + X)/dx_B$ as a function of x_B for model I. Different values of the Higgs boson mass is considered, i.e. $m_{H^+} = 80, 100$ and 120 GeV. Other free parameter is fixed to $\tan\beta = 5$.

the assumed top quark mass and may also depend on M_{SUSY} (the soft SUSY breaking scale parameter).

In Fig. 1, Both the b-quark and gluon fragmentations are included. In Ref. [7], we showed the $g \rightarrow B$ contribution is negative and appreciable only in the low- x_B region. For higher values of x_B the NLO result is practically exhausted by the $b \rightarrow B$ contribution.

From Fig. 1, it can be seen that when $\tan\beta$ is increased the decay rate is decreased and the peak position is shifted towards higher values of x_B . In Ref. [14], it is shown when the values of $\tan\beta$ exceed $\tan\beta = 2$, the decay rate becomes quite small. Here, the mass of B-hadron creates a threshold at $x_B = 2m_B/(m_t(1 + R - y)) = 0.12$.

Adopting the limit $80\text{GeV} \leq m_{H^\pm} \leq 160\text{GeV}$ from Ref. [22], in Fig. 2 we study the energy spectrum of the B-hadron for model I in different values of the Higgs boson mass, i.e. $m_{H^+} = 80, 100$ and 120 GeV, by fixing $\tan\beta = 5$. As mentioned, the mass of B-hadron is responsible for the thresholds at $x_B = 0.08$ (for $m_{H^+} = 80$ GeV), $x_B = 0.09$ (for $m_{H^+} = 100$ GeV) and $x_B = 0.12$ (for $m_{H^+} = 120$ GeV).

In Fig. 3 and Fig. 4, the results presented in Figs. 1 and 2 are regained for model II. The thresholds are as before.

In Fig. 5, we compared the energy spectrum of B-hadron in the GM-VFN ($m_b \neq 0$) and ZM-VFN ($m_b = 0$) schemes, using $\tan\beta = 1$ and $m_{H^+} = 120$ GeV. As it is shown, the results of both models are the same in the GM-VFN scheme but the result of ZM-VFN scheme shows an enhancement in the size of decay rate about 1.3% at $x_B = 0.8$. In Figs. 6

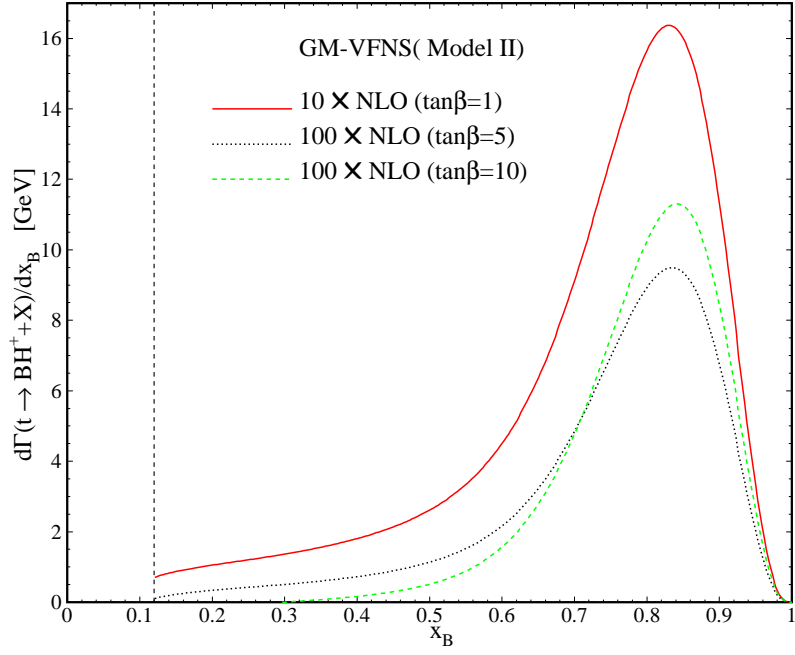


Figure 3. x_B spectrum in top decay considering the decay mode $t \rightarrow BH^+ + X$, taking $m_{H^+} = 120$ GeV and $\tan\beta = 1, 5$ and 10 in model II. Threshold at x_B is shown.

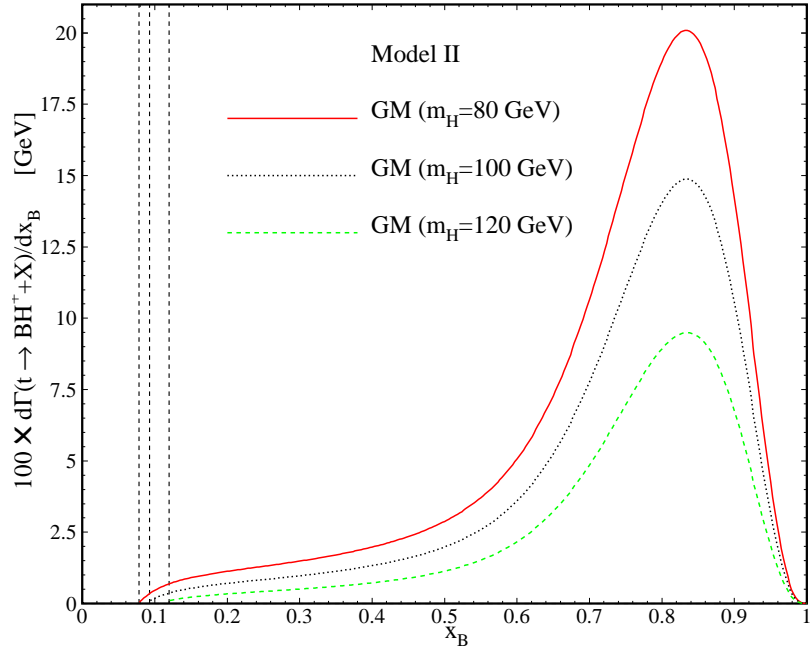


Figure 4. x_B spectrum for model II considering the different values of the Higgs boson mass, i.e. $m_{H^+} = 80, 100$ and 120 GeV, by fixing $\tan\beta = 5$.

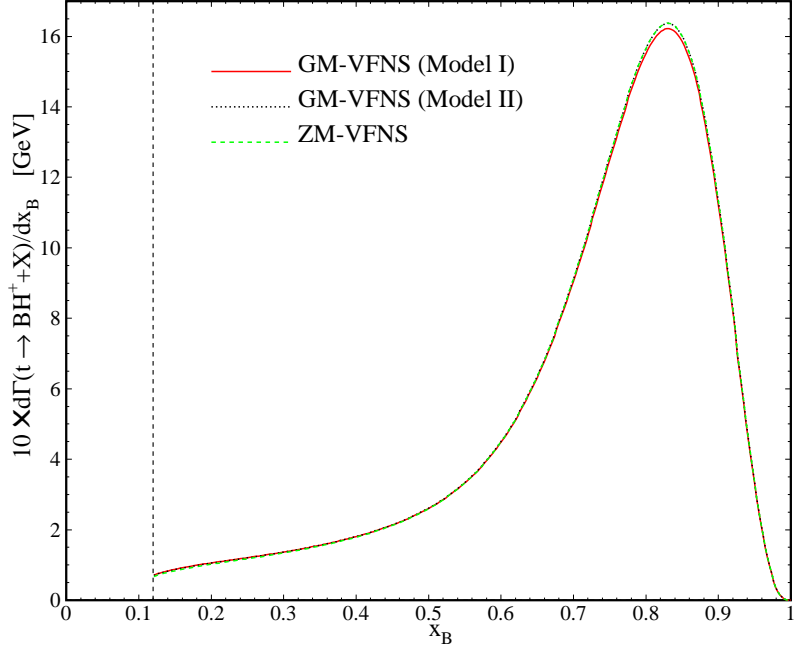


Figure 5. $d\Gamma(t \rightarrow B + H^+)/dx_B$ as a function of x_B at NLO. The GM-VFNS results in two models are compared to the ZM-VFNS scheme using $m_{H^+} = 120$ GeV and $\tan\beta = 1$.

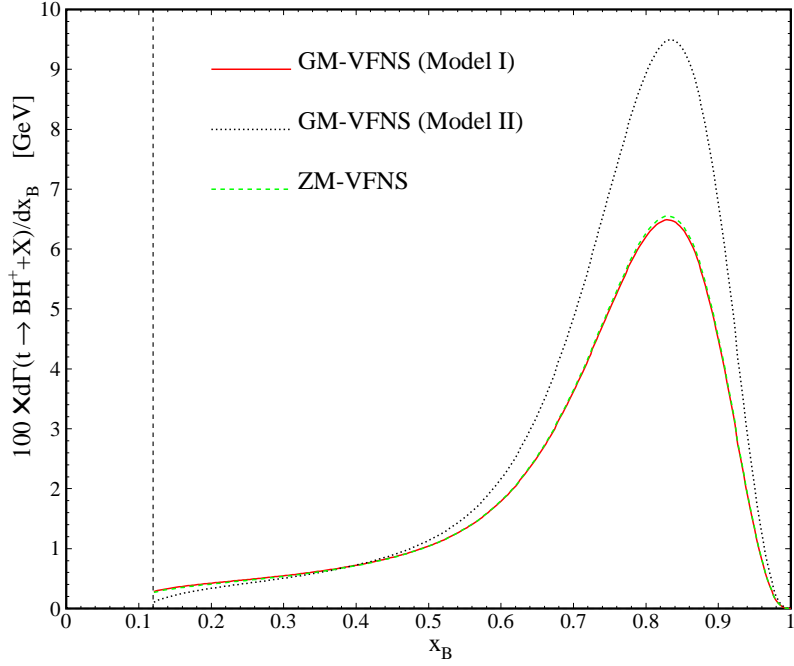


Figure 6. As in Fig. 5, but using $\tan\beta = 5$.

and 7, this comparison is done using $\tan\beta = 5, 10$ and $m_{H^+} = 120$ GeV. As it is seen,

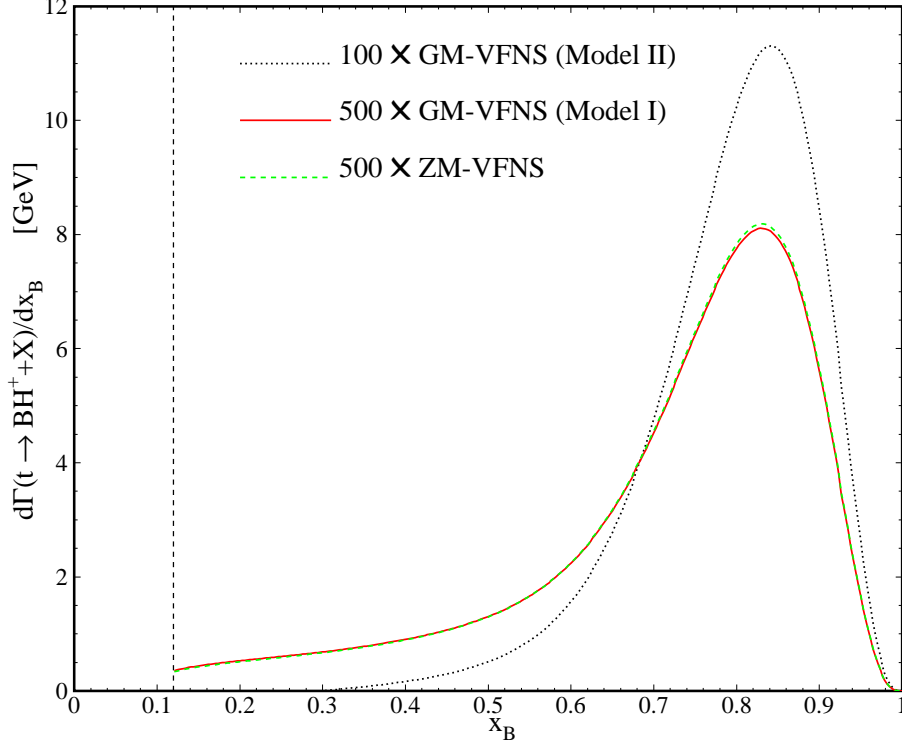


Figure 7. x_B spectrum at NLO as Figs. 5 and 6 but using $\tan \beta = 10$.

the prediction for the energy spectrum extremely depends on the model at the large values of $\tan \beta$ when $m_b \neq 0$. Therefore, our most reliable prediction for the energy spectrum is made at NLO in the GM-VFN scheme.

In Fig. 8, the energy spectrum of B-hadron in decay modes $t \rightarrow BW^+ + X$ and $t \rightarrow BH^+ + X$ are compared. As before, the mass of B-hadron create the thresholds at $x_B = 0.12$ (for $m_{H^+} = 120$ GeV) and $x_B = 0.08$ (for $m_{W^+} = 80.399$ GeV). It is obvious that the contribution of the top decay mode in the SM is always larger than the one coming from the 2HDM. However, to obtain the total energy spectrum of B-hadron in the top quark decay all decay modes including $t \rightarrow B + W^+/H^+$ should be summed up.

5 Conclusions

Clearly, the decay modes $t \rightarrow W^+ + B$ have been and will be the prime source of information on the top quark mass. We have studied these dominant decay modes along the lines of Ref. [4]. In the theories beyond the standard model including the two-Higgs-doublet, the top quarks also decay into a charged Higgs and a bottom quark thus it may be useful to also use $t \rightarrow H^+ + B$ events for a cross check. The search for the light charged Higgs boson ($m_{H^+} < m_t$) produced from the decay mode $t \rightarrow bH^+ (\rightarrow \tau^+ \nu)$ has been performed using about $1fb^{-1}$ of data collected in proton-proton collisions at $\sqrt{s} = 7$ TeV [5].

In our previous work [7], we applied the ZM-VFN scheme to study the dominant decay

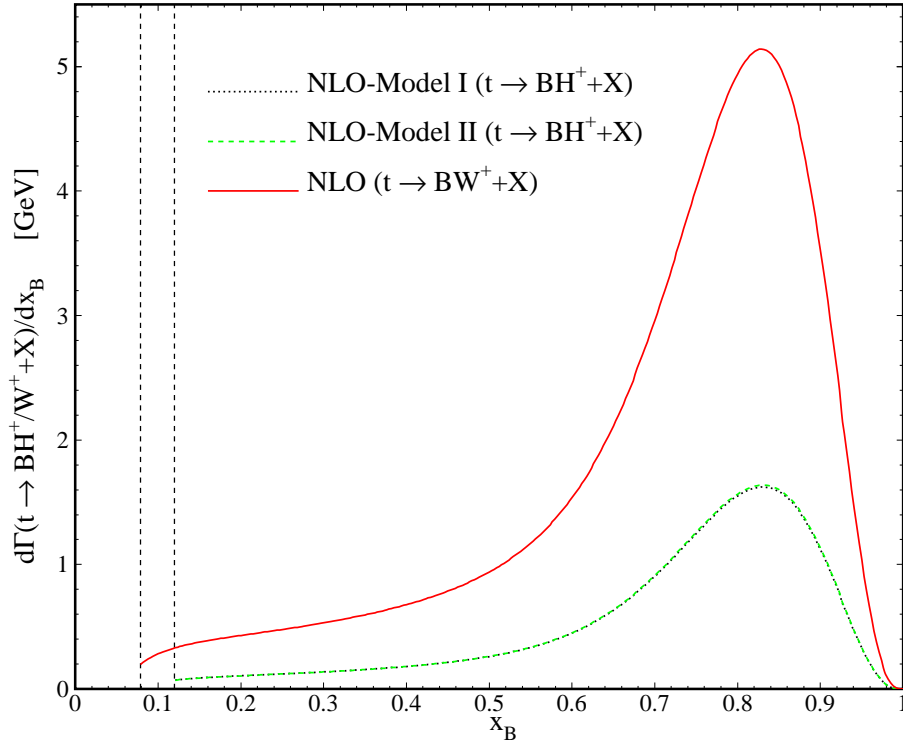


Figure 8. x_B spectrum in top decay considering the decay modes $t \rightarrow BW^+ + X$ (solid line) and $t \rightarrow BH^+ + X$ (dashed and dotted lines), taking $m_{W^+} = 80.399$ GeV, $m_{H^+} = 120$ GeV and $\tan \beta = 1$.

channel $t \rightarrow BH^+ + X$ in the 2HDM, where the mass of bottom-quark was set to zero and thus all information on the m_b dependence of the B-hadron spectrum was wasted. In the present work, we studied the energy spectrum of B-hadron in top decay considering the quantity $d\Gamma/dx_B$ in GM-VFN scheme. Our main purpose was to investigate both the effect of b-quark mass and the gluon fragmentation to the B-hadron energy distribution. In order to study these effects we have calculated, for the first time, an analytic expression for the NLO radiative corrections to the differential top decay width $d\tilde{\Gamma}/dx_a$ ($a = b, g$) in two variants of the 2HDM. To ensure our results, we have checked that by integrating $d\tilde{\Gamma}/dx_b$ over x_b we recover the known results presented in Refs. [14, 15].

In Ref. [7], we showed in the limit $m_b \rightarrow 0$ our results in both models are the same but in the present work we have checked the results for the energy spectrum of B-hadron are completely different for two models in the general 2HDM when $m_b \neq 0$ and $\tan \beta$ is large. In conclusion, the most reliable predictions for $d\Gamma/dx_B$ is made at NLO in the GM-VFN scheme.

Comparing future measurements of $d\Gamma/dx_B$ at the LHC with the presented predictions will be important for our understanding of the Higgs coupling in 2HDM and new physics beyond the standard model. Our results in Refs. [4, 7] and the present work both will be able to test the universality of the B-hadron fragmentation functions and provide a clean method

to gauge the normalization of Monte Carlo event generators.

Acknowledgments

I would like to thank Professor Bernd Kniehl for reading the manuscript and also for his important comments. I would also like to thank Dr Mathias Butenschon for reading and improving the manuscript. This work was supported by Yazd university and the Institute for Research in Fundamental Science (IPM).

References

- [1] Tevatron EW Working Group and CDF & D0 Collaboration, arXiv:0903.2503 [hep-ex].
- [2] U. Langenfeld, S. Moch, P. Uwer, arXiv:0907.2527 [hep-ph].
- [3] N. Cabibbo, Phys. Rev. Lett. **10**, 531 (1963); M. Kobayashi and T. Maskawa, Prog. Theor. Phys. **49**, 652 (1973).
- [4] B. A. Kniehl, G. Kramer and S. M. M. Nejad, Nucl. Phys. B **862**, 720 (2012) arXiv:1205.2528 [hep-ph].
- [5] A. Djouadi, Phys. Rept. **459**, 1 (2008) [hep-ph/0503173].
- [6] J. F. Gunion and H. E. Haber, Nucl. Phys. B **272**, 1 (1986); **402**, 567 (1993).
- [7] S. M. Moosavi Nejad, Phys. Rev. D **85**, 054010 (2012).
- [8] A. Ali, F. Barreiro and J. Llorente, Eur. Phys. J. C **71**, 1737 (2011).
- [9] ATLAS Collaboration, *Search for charged Higgs bosons in the τ +jets final state in $t\bar{t}$ decays with 1.03fb^{-1} of pp collision data recorded at $\sqrt{s} = 7\text{ TeV}$ with the ATLAS experiment*, ATLAS-CONF-2011-138 (2011)
- [10] V. N. Gribov and L. N. Lipatov, Sov. J. Nucl. Phys. **15**, 438 (1972) [Yad. Fiz. **15**, 781 (1972)]; G. Altarelli and G. Parisi, Nucl. Phys. **B126**, 298 (1977); Yu. L. Dokshitzer, Sov. Phys. JETP **46**, 641 (1977) [Zh. Eksp. Teor. Fiz. **73**, 1216 (1977)].
- [11] G. Corcella and A. D. Mitov, Nucl. Phys. B **623**, 247 (2002).
- [12] G. Corcella and F. Mescia, Eur. Phys. J. C **65**, 171 (2009); **68**, 687(E) (2010); S. Biswas, K. Melnikov, and M. Schulze, J. High Energy Phys. 08 (2010) 048.
- [13] J. F. Gunion, H. Haber, G. Kane, and S. Dawson, *The Higgs Hunter's Guide* (Addison-Wesley, Reading, MAA, 1990), and references therein.
- [14] A. Kadeer, J. G. Körner, and M. C. Mauser, Eur. Phys. J. C **54**, 175 (2008).
- [15] A. Czarnecki and S. Davidson, Phys. Rev. D **47**, 3063 (1993).
- [16] J. Liu and Y. P. Yao, Phys. Rev. D **46**, 5196 (1992).
- [17] S. Dittmaier, Nucl. Phys. B **675**, 447 (2003).
- [18] J. C. Collins, Phys. Rev. D **58**, 094002 (1998).
- [19] B. A. Kniehl, G. Kramer, I. Schienbein and H. Spiesberger, Phys. Rev. D **71**, 014018 (2005).
- [20] B. A. Kniehl, G. Kramer, I. Schienbein and H. Spiesberger, Phys. Rev. Lett. **96**, 012001 (2006).

- [21] B. Mele, P. Nason, Nucl. Phys. B 361 (1991) 626;
J.P. Ma, Nucl. Phys. B 506 (1997) 329;
S. Keller, E. Laenen, Phys. Rev. D 59 (1999) 114004;
M. Cacciari, S. Catani, Nucl. Phys. B 617 (2001) 253;
K. Melnikov, A. Mitov, Phys. Rev. D 70 (2004) 034027;
A. Mitov, Phys. Rev. D 71 (2005) 054021.
- [22] A. Ali, E. A. Kuraev and Y. M. Bystritskiy, Eur. Phys. J. C **67**, 377 (2010).
- [23] B. Abbott *et al.* [D0 Collaborations], Phys. Rev. Lett. **82**, 4975 (1999).
- [24] A. Abulencia *et al.* [CDF Collaboration], Phys. Rev. Lett. **96**, 042003 (2006).
- [25] G. Aad *et al.* [ATLAS Collaboration], JINST **3**, S08003 (2008).
- [26] K. Nakamura *et al.* (Particle Data Group), J. Phys. G **37**, 075021 (2010).
- [27] A. Heister *et al.* (ALEPH Collaboration), Phys. Lett. B **512**, 30 (2001).
- [28] G. Abbiendi *et al.* (OPAL Collaboration), Eur. Phys. J. C **29**, 463 (2003).
- [29] K. Abe *et al.* (SLD Collaboration), Phys. Rev. Lett. **84**, 4300 (2000); Phys. Rev. D **65**, 092006 (2002); **66**, 079905 (2002).
- [30] B. A. Kniehl, G. Kramer, I. Schienbein, and H. Spiesberger, Phys. Rev. D **77**, 014011 (2008).
- [31] B. Abbott *et al.* (DØ Collaboration), Phys. Rev. D **58**, 052001 (1998); T. Affolder *et al.* (CDF Collaboration), Phys. Rev. D **63**, 032003 (2001).
- [32] S. Schael *et al.* [ALEPH and DELPHI and L3 and OPAL and LEP Working Group for Higgs Boson Searches Collaborations], Eur. Phys. J. C **47**, 547 (2006).